

# Catalytic Consequences of Composition in Polyoxometalate Clusters with Keggin Structure\*\*

Josef Macht, Michael J. Janik, Matthew Neurock, and Enrique Iglesia\*

Reliable correlations among structure, composition, and function in heterogeneous catalysis require well-defined atomic connectivity within active structures and the assessment of the specific elementary steps and reaction intermediates responsible for the relevant catalytic function. The non-uniform nature of typical active structures creates significant challenges because probes of structure and function average such heterogeneity in complex ways. Polyoxometalate (POM) clusters with stable Keggin structures and well-defined atomic connectivity provide the compositional diversity required for a rigorous assessment of the consequences of composition on catalytic reactivity.

We describe herein the effects of the central atom X (P, Si, Al, and Co) in Keggin-type POM clusters ( $H_{8-n}X^{n+}W_{12}O_{40}$ ;  $H_{8-n}XW$ ) on acid strength based on calculated deprotonation enthalpies, which reflect intrinsic acid strength, and reactivity, based on a rigorous analysis of elementary rate constants, using 2-butanol dehydration as a probe reaction. Previous studies have not reported intrinsic acid properties for these materials and treated reactivity merely in terms of measured rates without the mechanistic interpretations required for meaningful composition–function relations.<sup>[1]</sup>

The ubiquitous aggregation and incomplete and environment-dependent accessibility<sup>[2,3]</sup> of POM clusters was minimized by dispersing them onto  $SiO_2$  supports. The number of accessible protons, required for rigorous measurements of turnover rates, was determined by titration with pyridine during catalysis. We conclude that C–O bond breaking in chemisorbed butanol monomers is the kinetically relevant step, while butanol dimers that form by solvation of adsorbed

butanol with another butanol molecule are unreactive spectators. Measured turnover rates depend on the rate constant for C–O cleavage and on the equilibrium constant for dimer formation; their values were obtained from the measured effects of 2-butanol pressure on dehydration rates. Both constants increased with increasing valence of the central atom, as the deprotonation enthalpy—a measure of the relative stability of the conjugate base—decreased.

Supported POM clusters catalyze 2-butanol dehydration at low temperatures (333–373 K) without detectable deactivation or structural changes. Reaction rates decreased sharply with increasing 2-butanol pressure (Figure 1) on all POM

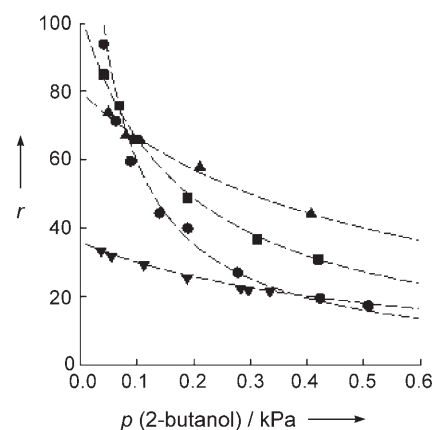


**Figure 1.** 2-Butanol dehydration rate  $r$  (in  $10^{-3}$  molecules 2-butanol  $POM^{-1} s^{-1}$ ) as a function of 2-butanol pressure for 0.04  $H_3PW/Si$  (●), 0.04  $H_5SiW/Si$  (■), 0.04  $H_5AlW/Si$  (▲), and 0.04  $H_6CoW/Si$  (▼) (343 K, 0.04  $POM\ nm^{-2}$ , conversion < 10%).

catalysts, as reported also for ethanol dehydration on bulk crystalline  $H_3PW_{12}$ .<sup>[4]</sup> This behavior reflects solvation of reactive  $C_2H_5OH_2^+$  intermediates to form less-reactive  $(C_2H_5OH)_2H^+$  dimers. <sup>13</sup>C NMR and infrared spectra, and ethanol uptakes confirmed these conclusions.<sup>[4,5]</sup> The measured kinetic response for 2-butanol dehydration also reflects the formation of unreactive co-adsorbed 2-butanol dimers. Theoretical estimates of the enthalpy of formation of butanol dimers by interactions of butanol with a monomer ( $-88.1\ kJ\ mol^{-1}$  for  $H_3PW$ ) confirmed the stable and unreactive nature of such dimers.

The identity of the central atom influenced 2-butanol dehydration rates on  $SiO_2$ -supported POM clusters (0.04  $H_{8-n}XW/Si$ ; 0.04  $POM\ nm^{-2}$  surface density; Figure 1). At 2-butanol pressures below 0.1 kPa, dehydration rates decreased in the sequence:  $H_3PW > H_5SiW > H_5AlW > H_6CoW$ , whereas these trends were essentially reversed at

[\*] J. Macht, Prof. E. Iglesia  
Department of Chemical Engineering  
University of California at Berkeley  
Berkeley, CA 94720 (USA)  
Fax: (+1) 510-642-4778  
E-mail: igelesia@berkeley.edu

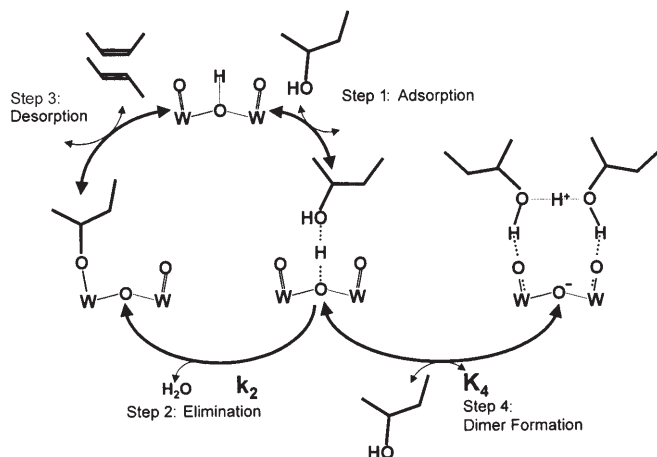
Prof. M. J. Janik  
Department of Chemical Engineering  
Pennsylvania State University  
University Park, PA 16802 (USA)  
Prof. M. Neurock  
Department of Chemical Engineering, University of Virginia  
Charlottesville, VA 22904 (USA)

[\*\*] Support by the Chemical Sciences, Geo Sciences, Bio Sciences Division, Office of Basic Energy Sciences, Office of Science US Department of Energy under grant number DE-FG02-03ER15479 is gratefully acknowledged. We also thank Dr. Cindy Yin for the synthesis of bulk  $H_5AlW$  and  $H_6CoW$  samples.

Supporting information for this article is available on the WWW under <http://www.angewandte.org> or from the author.

higher pressures ( $H_5AlW > H_4SiW > H_6CoW > H_3PW$ ). Thus, composition–function relations and the underlying effects of acid strength cannot be discerned by mere inspection of these rates, without their rigorous interpretation in terms of rate and equilibrium constants for elementary steps.

A plausible sequence of elementary steps includes 2-butanol adsorption on Brønsted acid sites, its irreversible decomposition through E1 or E2 elimination pathways, the reversible desorption of butene isomers, and the formation of unreactive protonated dimers (Scheme 1). At low conver-



**Scheme 1.** Proposed sequence of elementary steps for 2-butanol dehydration on POM clusters with Keggin structure.

sions, water coadsorption does not influence measured rates because of the large excess of 2-butanol and the lower adsorption energies calculated for  $H_2O$  ( $-67 \text{ kJ mol}^{-1}$ ) relative to 2-butanol monomers ( $-77 \text{ kJ mol}^{-1}$ ).

Elimination can occur through E1 or E2 pathways.<sup>[6,7]</sup> E2 routes involve concerted cleavage of C–O and C–H bonds in butanol monomers using acid–base pairs and form one butene molecule, one OH group, and adsorbed water which is subsequently desorbed. E1 pathways cleave C–O bonds to form water molecules and adsorbed butoxides; the latter undergo H-abstraction and desorb as butene isomers. On  $0.04H_3PW/Si$ , the *cis/trans* ratios in 2-butenes formed by 2-butanol dehydration and through 1-butene (double-bond isomerization; extrapolated to zero conversion) are similar (0.95 vs. 0.97) and much larger than the thermodynamic value (0.40). These similar stereoselectivities reflect a common *sec*-butyl alkoxide intermediate as the source of butenes in these two reactions, and indicate the prevalence of E1 routes that involve them. 1-Butene isomerization rates were much larger ( $0.8 \text{ (POMs)}^{-1}$ ) than 2-butanol dehydration rates ( $0.02\text{--}0.09 \text{ (POMs)}^{-1}$ ) at 343 K on  $0.04H_3PW/Si$ , indicating that H-elimination from butoxide intermediates, required also in double-bond isomerization turnovers, occurs much faster than butene formation by 2-butanol dehydration. Thus, the step that forms these butoxide intermediates (C–O cleavage in E1 pathways) must be the kinetically relevant step in dehydration catalysis. DFT calculations also indicate that C–O cleavage is kinetically relevant and that reactions occur through carbenium ion transition states stabilized by inter-

actions with the anionic Keggin structure (Figure 2). The calculated activation energy for C–O bond breaking is  $132 \text{ kJ mol}^{-1}$  ( $H_3PW$ ), whereas the 2-butene desorption activation energy is significantly lower ( $88 \text{ kJ mol}^{-1}$ ). The level of

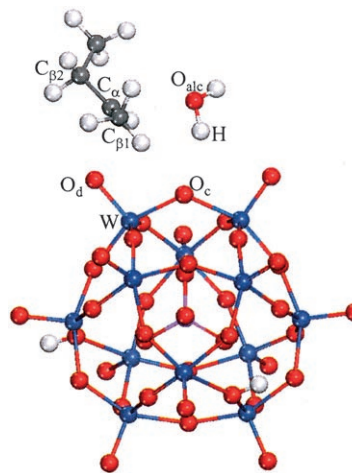


**Figure 2.** DFT-calculated transition state for 2-butanol dehydration on  $H_3PW$  to a *sec*-butyl alkoxide and a weakly bound water molecule.

substitution at the carbon atom bearing the OH group, increased by using 1-butanol, 2-butanol, and *tert*-butanol as reactants, markedly increased the dehydration rates ( $k_{1\text{-butanol}}:k_{2\text{-butanol}}:k_{\text{tert-butanol}} = 1:2000:1 \times 10^5$  (343 K)), consistent with the kinetic relevance of C–O bond cleavage and with the ionic character of the E1 elimination transition state.

The elementary steps in Scheme 1 lead, with the assumptions of a quasi-equilibrated step 4 and adsorbed 2-butanol (step 1) and 2-butanol dimers (step 4) as most abundant surface species, to Equation (1) for rates measured at low conversions (see Supporting Information for derivation).

$$r = \frac{k_2[H^+]}{1 + K_4[C_4H_9OH]} \quad (1)$$

The  $k_2$  and  $K_4$  terms represent the 2-butanol decomposition rate constant and the equilibrium constant for dimer formation, respectively (Scheme 1), and  $[H^+]$  is the number of accessible proton sites. Equation (1) accurately describes the pressure dependence of measured rates, as shown by the linear dependence of inverse rates on 2-butanol pressure (Figure 39). At low 2-butanol pressures ( $< 0.1 \text{ kPa}$ ), the value of  $k_2[H^+]$  determines dehydration rates; at higher 2-butanol pressures, rates depend on  $(k_2[H^+])/K_4$ . As a result, the ranking of catalysts and the role of central atom and of acid strength are substantially different at high and low reactant pressures.

A regression analysis of the pressure dependence of dehydration rates (per POM) gave accurate estimates for  $k_2[H^+]$  and  $K_4$ .  $[H^+]$  values were determined by titration with pyridine during the catalytic reaction, because accessibility constraints within secondary POM structures can depend sensitively on the size and polarity of reactants and products.<sup>[2,3]</sup> The number of accessible protons sites  $[H^+]$  was

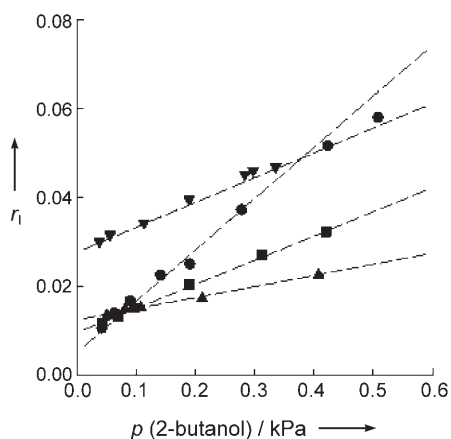


**Figure 3.** Inverse 2-butanol dehydration rate  $r_1$  (in  $10^3$  POM s (molecules 2-butanol) $^{-1}$ ) as a function of 2-butanol pressure for 0.04 H<sub>3</sub>PW/Si (●), 0.04 H<sub>4</sub>SiW/Si (■), 0.04 H<sub>5</sub>AlW/Si (▲), and 0.04 H<sub>6</sub>CoW/Si (▼) (343 K, 0.04 POM nm $^{-2}$ , conversion < 10%).

similar to that expected from stoichiometry in all samples (e.g. 0.04 H<sub>3</sub>PW<sub>12</sub>/Si, 2.9 [H<sup>+</sup>] measured; Table 1), consistent with intact clusters and with weak interactions between protons and silanols on silica surfaces.

**Table 1:** Proton site density [H<sup>+</sup>], alkoxy formation rate constant  $k_2$ , and the 2-butanol dimer formation equilibrium constant  $K_4$  (see Scheme 1) for 2-butanol dehydration on 0.04 H<sub>8-n</sub>X<sup>n+</sup>W/Si.<sup>[a]</sup>

	[H <sup>+</sup> ] (per POM) <sup>[b]</sup>	$k_2$ [10 $^{-3}$ (s H <sup>+</sup> ) $^{-1}$ ] <sup>[c]</sup>	$K_4$ [kPa $^{-1}$ ] <sup>[c]</sup>
0.04 H <sub>3</sub> PW/Si	2.9	60.3	21
0.04 H <sub>4</sub> SiW/Si	3.8	28.7	6
0.04 H <sub>5</sub> AlW/Si	5	16.0	2
0.04 H <sub>6</sub> CoW/Si	6	6.0	2

[a] X = P<sup>5+</sup>, Si<sup>4+</sup>, Al<sup>3+</sup>, and Co<sup>2+</sup>; 0.04 POM nm $^{-2}$  surface density; 343 K, 101 kPa He, 0.05–0.6 kPa 2-butanol. [b] Determined by titration with pyridine during 2-butanol dehydration reaction (343 K, 0.5 kPa 2-butanol, 0.9 Pa pyridine). [c] Determined by fitting Eq. (1) to the experimental data.

Both  $k_2$  and  $K_4$  decreased in parallel with decreasing oxidation state of X in H<sub>8-n</sub>XW<sub>12</sub> clusters (P > Si > Al > Co, Table 1) and as the number of charge-balancing protons increased. Activation barriers calculated for C–O cleavage in 2-butanol and dimer formation energies from DFT follow trends with central atom similar to those measured experimentally. The observed trends in  $k_2$  and  $K_4$  values parallel the effects of central atom on the enthalpy for removing the first proton from H<sub>8-n</sub>XW<sub>12</sub> clusters (Figure 4, and Table 2). The deprotonation enthalpy is defined as that for AH → A<sup>−</sup> + H<sup>+</sup> (AH is the neutral cluster; A<sup>−</sup> is the deprotonated conjugate base). Deprotonation enthalpies were calculated using density functional theory (DFT);<sup>[8]</sup> they reflect the relative stability of the conjugate base and the intrinsic acid strength of the neutral cluster. These enthalpies increased (1087 kJ mol $^{-1}$  (H<sub>3</sub>PW), 1143 kJ mol $^{-1}$  (H<sub>6</sub>CoW)), and the conjugate base became less stable, as the oxidation state of the central atom X decreased and the number of protons per

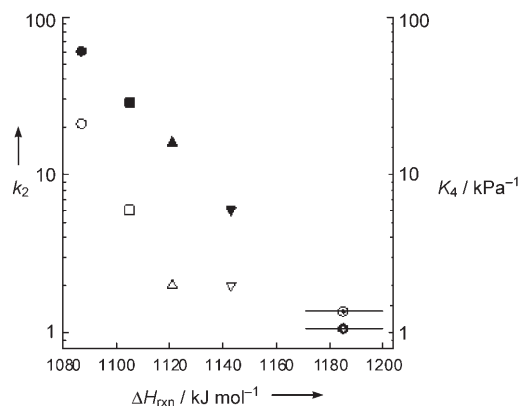


**Figure 4.** 2-Butanol decomposition rate constant  $k_2$  (in  $10^{-3}$  molecules 2-butanol (H<sup>+</sup>) $^{-1}$  s $^{-1}$ ) (closed symbols) and dimer formation equilibrium constant  $K_4$  (open symbols) as a function of deprotonation enthalpy, defined as  $\Delta H_{\text{rxn}}$  of HA → A<sup>−</sup> + H<sup>+</sup> (HA is the acid, and A<sup>−</sup> is the conjugate base) and calculated by DFT. (0.04 H<sub>3</sub>PW/Si (●), 0.04 H<sub>4</sub>SiW/Si (■), 0.04 H<sub>5</sub>AlW/Si (▲), 0.04 H<sub>6</sub>CoW/Si (▼), and H-BEA (◆)). — denotes the deprotonation energy range reported for different zeolite catalysts.<sup>[10]</sup>

**Table 2:** DFT-calculated deprotonation enthalpies DPE ( $\Delta H_{\text{rxn}}$  of HA → A<sup>−</sup> + H<sup>+</sup>), activation energies for the alkoxy formation step ( $E_{\text{a2,calcd}}$ ), and 2-butanol dimer formation enthalpies ( $\Delta H_{\text{4,calcd}}$ ) (see Scheme 1) for 2-butanol dehydration on H<sub>8-n</sub>X<sup>n+</sup>W/Si.

	DPE <sup>[b]</sup>	$E_{\text{a2,calcd}}$ <sup>[b]</sup>	$\Delta H_{\text{4,calcd}}$ <sup>[b]</sup>
H <sub>3</sub> PW	1087	132.4	83.7
H <sub>4</sub> SiW	1105	140.0	76.7
H <sub>5</sub> AlW	1121	145.8	70.3

[a] HA is the acid, and A<sup>−</sup> is the conjugate base; X = P<sup>5+</sup>, Si<sup>4+</sup>, and Al<sup>3+</sup>. [b] In kJ mol $^{-1}$ .

cluster concurrently increased. Deprotonation enthalpies rigorously rank solid Brønsted acids in terms of their acid strength. The values estimated by DFT suggest that Keggin-type POM clusters (1087–1143 kJ mol $^{-1}$ ) are stronger acids than H<sub>2</sub>SO<sub>4</sub> (1293 kJ mol $^{-1}$ ) and CF<sub>3</sub>SO<sub>3</sub>H (1248 kJ mol $^{-1}$ ) and comparable to the CB<sub>11</sub>H<sub>12</sub>H carborane acid (1084 kJ mol $^{-1}$ ).<sup>[9]</sup>

The values of  $k_2$  and  $K_4$  were similarly affected by POM deprotonation enthalpy because butyl carbenium ion transition states and unreactive protonated 2-butanol dimers are significantly ionic in character and benefit from the effective delocalization of the concomitant negative charge by POM clusters.<sup>[8]</sup> In contrast, charge is highly localized on inorganic insulators, such as the silicate framework in zeolites, and deprotonation enthalpies are significantly higher for zeolites (ranging from 1171 (zeolite Y) to 1200 kJ mol $^{-1}$  (ZSM-5))<sup>[10]</sup> than for POM clusters. On H-BEA, the higher deprotonation enthalpy led also to lower  $k_2$  and  $K_4$  values; these data fell on the same correlation with deprotonation enthalpy as the various H<sub>8-n</sub>XW clusters (Figure 4). We note that the range of deprotonation enthalpies among various zeolite structures (Y, CHA, MOR, MFI) (1171–1200 kJ mol $^{-1}$ ; 29 kJ mol $^{-1}$  range)<sup>[10]</sup> is smaller than for the various POM structures reported herein (1087–1143 kJ mol $^{-1}$ ; 56 kJ mol $^{-1}$  range). POM clusters

therefore provide a greater range of acid strengths useful in the practice of Brønsted acid catalysis.

The central atom strongly influences the reactivity of protons in Keggin-type POM clusters through the combined effects on the rate constant of C–O bond breaking  $k_2$  and the equilibrium constant for the formation of unreactive 2-butanol dimers  $K_4$ . Both increased in parallel as the oxidation state of the central atom X in  $H_{8-n}X^{n+}W$  increased (Co < Al < Si < P) and the deprotonation enthalpy concurrently decreased, because of the ionic character of the transition state in C–O cleavage and of the 2-butanol dimer. Reaction rates reflect  $k_2$  and  $K_4$  values in a manner that leads to compensating effects and to rates that benefit from stronger acids at low butanol pressures but from weaker acids at higher pressures. 2-Butanol dehydration rates (at 0.5 kPa 2-butanol pressure) increased by a factor of 2.6 as deprotonation enthalpies decreased by  $34 \text{ kJ mol}^{-1}$  ( $H_5AlW \rightarrow H_3PW$ ; Figure 1).

Earlier, van Santen and Kramer proposed, based on electronic structure calculations, a relation between the stability of cationic species present as transition states and the deprotonation energies of Brønsted acids.<sup>[11]</sup> Our study provides experimental verification for this proposal for the dehydration of 2-butanol on POM clusters in terms of a rigorous analysis of turnover rates in terms of rate and equilibrium constants for elementary steps. The relationship between the stability of transition states and of intermediates and the intrinsic acid strength is essential to design materials with specific reactivity and selectivity in acid catalysis. Indeed, activation barriers for steps involving ionic transition states benefit from lower deprotonation enthalpies, but these steps may not limit overall catalytic rates. Deprotonation enthalpies also influence the stability of ionic intermediates of varying reactivity, leading to compensating effects that cause rates that increase or decrease with increasing deprotonation enthalpy depending on the relative concentrations of reactive and unreactive intermediates.

### Experimental Section

$H_3PW_{12}O_{40}$  (Aldrich),  $H_4SiW_{12}O_{40}$  (Aldrich, 99.9%),  $H_5AlW_{12}O_{40}$  (prepared as in Ref. [12]), and  $H_6CoW_{12}O_{40}$  clusters (prepared as in Ref. [13,14]) were deposited onto  $SiO_2$  (Cab-O-Sil,  $304 \text{ m}^2 \text{ g}^{-1}$ , pore volume  $1.5 \text{ cm}^3 \text{ g}^{-1}$ ; washed three times in 1 M  $HNO_3$  and dried in Air (Praxair, extra-dry, 573 K, 5 h,  $20 \text{ cm}^3 \text{ g}^{-1}$ ) by incipient wetness impregnation with  $1.5 \text{ cm}^3$  of ethanol (Aldrich, anhydrous 99.5%)— $H_3PW$ ,  $H_4SiW$ ,  $H_5AlW$ , or  $H_6CoW$  solutions per gram of dry  $SiO_2$ . Impregnated samples were treated in flowing dry air (Praxair, extra-dry) at 323 K for 24 h. H-BEA (Zeolyst) with Si/Al 12.5:1 was used.

Catalytic 2-butanol dehydration rates and selectivities were measured at 343 K in a quartz flow cell (1.0 cm inner diameter) containing samples (1–100 mg of catalysts (125–180  $\mu\text{m}$ ) diluted with acid-washed quartz ( $\approx 50 \text{ mg}$ , 125–180  $\mu\text{m}$ )) held on a porous quartz disc. Temperatures were measured using K-type thermocouples and set using a Watlow controller (Series 982) and a resistively-heated furnace. Samples were treated in flowing He ( $80 \text{ cm}^3 \text{ min}^{-1}$ , Praxair, UHP (He), extra-dry (air)) at 343 K for 1 h before catalytic measurements. Thermal treatments in He or air ( $80 \text{ cm}^3 \text{ min}^{-1}$ , Praxair, UHP) at 373–575 K did not influence measured rates. Transfer lines were held at 393 K to prevent adsorption or condensation of reactants, products, and titrants before chromatographic analysis. Butanol

reactants (Sigma-Aldrich, 99.5% (2-butanol), 99.8% (1-butanol), 99.5% (*tert*-butanol, anhydrous)) were introduced as a liquid using a syringe pump (Cole Parmer, 74900 series) and vaporized at 393 K by injection into flowing He (Praxair, UHP). 1-Butene (Scott Specialty Gases, 99%) flow rates, liquid 2-butanol introduction rates and He flow rates were adjusted to give desired reactant pressures and to keep conversions low (< 10%) and relatively constant among various catalyst samples. Reactant and product concentrations were measured by gas chromatography using flame ionization detection (Agilent 6890N GC, 50 m HP-1 column). Only butene products of dehydration reactions were detected (1-butene, *cis*-2-butene, and *trans*-2-butene). Brønsted acid sites were titrated by introducing liquid mixtures of 2-butanol reactants (Sigma-Aldrich, 99.5%, anhydrous) with pyridine (Aldrich, 99.9%) into flowing He to give 0.5 kPa 2-butanol and 0.9 Pa pyridine. The amount of titrant adsorbed on the catalyst was measured from measurements of its concentration in the effluent stream using the chromatographic protocols described above for 2-butanol dehydration.

Calculations were carried out using a periodic plane wave density functional theory code VASP.<sup>[15,16]</sup> The generalized gradient approximation of the Perdew-Wang form (PW91) was used to correct exchange energies.<sup>[17]</sup> A cut off energy of 396.0 eV defined the plane wave basis set expansion and ultrasoft pseudopotentials<sup>[18]</sup> were used to model the electron–ion interactions. The Keggin structure was placed in the center of a  $20 \times 20 \times 20 \text{ \AA}^3$  supercell to allow for a sufficient vacuum region between neighboring Keggin structures. A single  $\Gamma$ -point was found to be sufficient to sample the first Brillouin zone.<sup>[8]</sup> All reported structures were optimized to force values below 0.05 eV per atom. The climbing nudged elastic band method was used to locate transition states.<sup>[19]</sup>

Received: March 23, 2007

Revised: July 25, 2007

Published online: September 7, 2007

**Keywords:** acid catalysis · alcohols · cluster compounds · dehydration · polyoxometalates

- [1] Hammett indicator methods (e.g. T. Okuhara, C. Hu, M. Hashimoto, M. Misono, *Bull. Chem. Soc. Jpn.* **1994**, *67*, 1186) and liquid phase acid dissociation values (e.g. I. V. Kozhevnikov, *Chem. Rev.* **1998**, *98*, 171; T. Okuhara, N. Mizuno, M. Misono, *Adv. Catal.* **1996**, *41*, 133; M. N. Timofeeva, *Appl. Catal. A* **2003**, *256*, 19, and references therein) are solvent dependent and thus no measures of intrinsic acid strength. None of the work summarized in the aforementioned review papers discusses the effect of central atom on the catalytic function in terms of the rates of specific elementary steps.
- [2] N. Mizuno, M. Misono, *Chem. Rev.* **1998**, *98*, 199.
- [3] M. Misono, N. Mizuno, K. Katamura, A. Kasai, K. Sakata, T. Okuhara, Y. Yoneda, *Bull. Chem. Soc. Jpn.* **1982**, *55*, 400.
- [4] K. Y. Lee, T. Arai, S. Nakata, S. Asoka, T. Okuhara, M. Misono, *J. Am. Chem. Soc.* **1992**, *114*, 2836.
- [5] The additional stability gained by the formation of  $[R1-O-H-O-R2]^+$  cationic hydrogen bonds is well known, see *Molecular Structure and Energetics, Vol. 4* (Eds.: J. F. Liebman, A. Greenberg), VCH, Weinheim, **1987**, pp. 74–142, and references therein. The well-known  $H_3O_2^+$  ion is another example.
- [6] H. Noller, K. Thomke, *J. Mol. Catal.* **1979**, *6*, 375.
- [7] S. Delsarte, P. Grange, *Appl. Catal. A* **2004**, *259*, 269.
- [8] B. B. Bardin, S. V. Bordawekar, M. Neurock, R. J. Davis, *J. Phys. Chem. B* **1998**, *102*, 10817; M. J. Janik, A. C. Kimberly, B. B. Bardin, R. J. Davis, M. Neurock, *Appl. Catal. A* **2003**, *256*, 51.
- [9] I. A. Koppel, P. Burk, I. Koppel, I. Leito, T. Sonoda, M. Mishima, *J. Am. Chem. Soc.* **2000**, *122*, 5114.
- [10] M. Brändle, J. Sauer, *J. Am. Chem. Soc.* **1998**, *116*, 5428.

- [11] R. A. van Santen, G. J. Kramer, *Chem. Rev.* **1995**, *95*, 637; A. M. Rigby, G. J. Kramer, R. A. van Santen, *J. Catal.* **1997**, *170*, 1.
- [12] J. J. Cowan, C. L. Hill, R. S. Reiner, I. A. Weinstock, *Inorg. Synth.* **2002**, *33*, 18.
- [13] L. C. W. Baker, T. P. McCutcheon, *J. Am. Chem. Soc.* **1956**, *78*, 4503.
- [14] L. C. W. Baker, B. Love, T. P. McCutcheon, *J. Am. Chem. Soc.* **1950**, *72*, 2374.
- [15] G. Kresse, J. Hafner, *Phys. Rev. B* **1993**, *47*, 558.
- [16] G. Kresse, J. Furthmüller, *Phys. Rev. B* **1996**, *54*, 11169.
- [17] J. P. Perdew, J. A. Chevary, S. H. Vosko, K. A. Jackson, M. R. Pederson, D. J. Singh, C. Fiolhais, *Phys. Rev. B* **1992**, *46*, 6671.
- [18] D. Vanderbilt, *Phys. Rev. B* **1990**, *41*, 7892.
- [19] G. Henkelman, B. P. Uberuaga, H. Jonsson, *J. Chem. Phys.* **2000**, *113*, 9901.
-